euronoise

Experimental and Numerical Investigation of the Acoustic Response of Multi-slit Bunsen Burners

Philip De Goey, Victor Kornilov, Ronald Rook and Jan Ten Thije Boonkkamp

Eindhoven Univesity of Technology, Den Dolech 2, 5600 MB Eindhoven, Netherlands
l.p.h.d.goey@tue.nl

The design and construction of combustion systems like central heating boilers is obstructed by acoustic problems because these are largely misunderstood, despite our increase in knowledge over the last decades. Current models for the phase of the transfer function of Bunsen-type flames, based on the kinematic behavior of the flame, completely miss the experimentally observed phase, unless the measured flow field is used in the model. In this paper we analyze numerical results of the steady flame form and flame transfer function obtained with detailed, two-dimensional numerical simulations of flames on multi-slit burners. The numerical model is validated with experiments of the flame shape (using chemiluminescence) and the flame transfer function (using OH luminescence for the heat release fluctuations and heated wire probe for the acoustic distortions). We subsequently study the influence of changes in mean flow velocity, slit width and distance between the slits on the transfer function, both numerically and experimentally. The experimentally observed effect of varying equivalence ratio on the flame transfer function is also analyzed. Good agreement is found which indicates the importance of predicting the influence of the flow on the flame and vice versa.

1 Introduction

Noise problems often arise in technical combustion systems like domestic gas boilers or gas turbines. These problems are related to the interaction of acoustic waves in the complete system with the flame. Acoustic waves could lead to fluctuations in the heat release of the flame, which could amplify the acoustic wave which leads again to an increase of the acoustic energy in the system, provided the Rayleigh criterion is satisfied. If this happens near eigenmodes of the system, this might lead to acoustic instability, observed through noise and possibly even system failure if the velocity and pressure amplitudes are very high.

The feedback mechanism between the acoustic field and the heat release fluctuations can have different origins. There are many ways to arrange this coupling depending on the specific form and burner type. Here, we will consider the response of fully premixed laminar Bunsen-type flames on multi-slit burners with fixed equivalence ratio to a fluctuating velocity field, resembling an acoustic wave. It is expected that these small flames on multi-slit burners display (1) an oscillating heat release rate due to flame surface area undulations, as in the case of a Bunsen burner, and (2) on top of that an oscillating heat loss rate to the burner near the flame foot area resembling the case of a flat flame stabilized on a surface burner. Together these phenomena are responsible for a fluctuating heat release which is visible in terms of the flame transfer function (TF). Knowledge of such 'generic' flame structures might give new insight in the field of turbulent flames as appearing for instance in gas turbines.

The acoustic response of Bunsen-type flames has been studied intensively over the years. Current state of the art is that there exists an essential discrepancy between experimental and theoretical results. Putnam's experiments [8] with many different systems in which a self-sustained acoustic instability can be observed forced him to conclude that there is a combustion process time lag and that this time delay is equal to a traveling time of gas particles from the burner outlet to the mean position in the flame zone. By nature this time lag is a 'system time delay', in other words, the flame effectively responds to a flow perturbation some time τ_0 after it is applied at the burner outlet. This observation has been verified in many experimental studies afterwards. Several models have been introduced to predict this behavior. A very simple analytical model for predicting the kinematics of axi-symmetric premixed Bunsen flames in a tube has been derived by Fleifil et al. [1]. This model is based on the dynamic G-equation. Compared to experiments, the global structure of the flame shape motion is captured but the resulting flame transfer function is unsatisfactory. The model predicts a phase for the transfer function which is asymptotically approaching $\pi/2$ for large frequencies, while experiments have shown a much larger phase. A number of improvements of the kinematic models have been investigated over the years but the experiment has not been reproduced unless a measured velocity field is used to compute the flame motion [10].

In this paper we will investigate the response of Bunsen-type flames on multi-slit burners, both experimentally and numerically. This configuration is chosen as it can be easily modeled in a two-dimensional geometry. A kinematic flame surface model will not be used, but rather a more complex model which includes the Navier-Stokes and transport equations for a two-dimensional flame on a burner, in which the full interaction between flame, flow and burner is taken into account. Results of the flame geometry (flame front motion), flow field pattern and acoustic transfer function of the flame are compared with experimental results. The present paper contains results related to a parametric study of the flame TF (measured and simulated), accompanied by examples of the comparison of the steady flame form. Results related to temporally and spatially resolved motion of the flame front and flow field will be presented elsewhere.

We have organized this paper as follows. The experimental configuration is presented in the next section, including the outline of the experiments performed. In Section 3, the model used in numerical simulations is presented. The comparison of experimental and numerical results is presented in Section 4. This contribution ends with a few conclusions.

2 Experimental method

The burner consists of a vessel with a flat perforated disc inserted on top of it (see Fig. 1(a)). The disc contains a series of 12 mm long rectangular slits, each of width d whereas l is the distance between adjecent slits. The pitch then equals $l + d$ and the porosity $\xi = d/(d + l)$.

The slits are perforated in a steel plate of 1.0 mm thickness. A mixture of methane and air at ambient conditions ($p = 1.0\,\text{atm}$ and $T = 293\,\text{K}$), with an equivalence ratio Φ and a velocity $\bar{u}$ (approaching bulk velocity below the plate, leading to an average velocity of $V = \bar{u}/\xi$ in the slit) is used to stabilize the steady flames. The burning velocity of the mixture is s_L. The burner plate reaches temperatures in the range of $100°C - 150°C$ due to the steady combustion. The gas flows are controlled with mass flow controllers (MFC) installed far enough from the burner to allow a perfect mixing and to avoid a possible acoustic influence on Φ and/or $\bar{u}_\text{u}$. To impose a flow velocity perturbation u', a loudspeaker operated by a pure tone generator was installed upstream in the mixture supply tube. To measure the flame heat release rate, the chemoluminescence intensity of OH^* was chosen as an appropriate indicator. To monitor the velocity oscillation a hot-wire anemometer was installed 10 mm upstream, just beneath a slit in the burner vessel (see Fig.1).

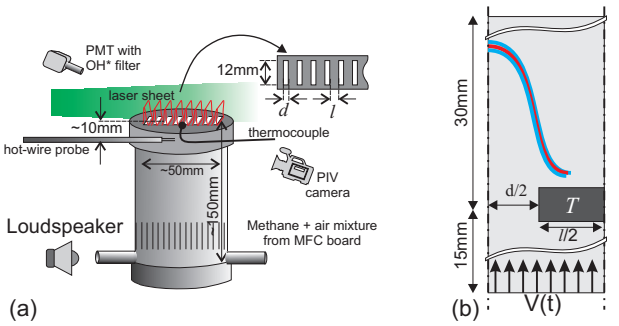

Figure 1: Burner setup (a) and calculation domain (b)

The response of the flame to acoustic waves is characterized in frequency domain by the so-called flame transfer function (TF), which is defined as the ratio of the relative heat release rate perturbation $q'/\bar{q}$ and the relative flow velocity perturbation $u'/\bar{u}$, i.e.,

$$\text{TF}(f) := \frac{q'/\bar{q}}{u'/\bar{u}}, \tag{1}$$

where f is the frequency of the velocity perturbation. The fluctuations q' are a result of flame surface variations due to flame front undulations and heat loss variations to the burner. Raw experimental data consist of 0.5 s samples of $u'(t)$ and $I'_{\text{OH}^*}(t)$ time histories digitized with a sampling rate of 20 kHz. The gain of the TF was calculated as the ratio of the amplitude of the Fourier transform of the $I'_{\text{OH}^*}(t)$ signal and the amplitude of the Fourier transform of the acoustic velocity signal $u'(t)$. The phase difference between $I'_{\text{OH}^*}(t)$ and $u'(t)$ was restored by a cross-correlation analysis of these signals. The TF can be presented either in the form of a frequency dependent gain $G(f)$ and phase delay $\phi(f)$ or in a polar plot where $G(f)$ presents the radial length and $\phi(f)$ presents the angle.

3 Numerical modeling

The code LAMFLA2D [4, 12] is used to simulate the response of methane-air flames to velocity perturbations. The code solves the primitive variable formulation of the conservation laws for two-dimensional, low-Mach number reacting flow. It is based on a one-step chemical reaction model for the species CH_4, O_2, CO_2, H_2O and N_2. LAMFLA2D uses the following numerical methods: a second order finite volume/complete flux scheme for space discretisation, the implicit Euler method for time integration, a pressure-correction method to decouple the pressure computation and a nonlinear multigrid method and GMRES to solve the discretised system. For more details see [4, 12, 13].

Most important details of the physical and chemical models used, are presented in the following. The diffusion fluxes are modeled using a Fick-like expression with the mixture-averaged diffusion coefficients given by

$$D_{i,\text{m}} = (1 - Y_i) / \sum_{j \neq i} X_j / D_{ij}, \tag{2}$$

where X_i and Y_i are the mole and mass fractions, respectively, and D_{ij} are the binary diffusion coefficients [11]. The transport equations are only solved for species CH_4, O_2, CO_2 and H_2O. The mass fraction of N_2, the N-th abundant species, is computed from $\sum_{i=1}^{N} Y_i = 1$ to assure that sum of fluxes is 0. A semi-empirical formulation is applied for the conductivity, i.e.,

$$\lambda = \frac{1}{2}\Big(\sum_{i=1}^{N} X_i \lambda_i + \Big(\sum_{i=1}^{N} X_i / \lambda_i \Big)^{-1} \Big), \tag{3}$$

where λ_i is the thermal conductivity of the ith species. The transport coefficients D_{ij} and λ_i are tabulated in terms of polynomial coefficients, similar as in the CHEMKIN package [6]. The thermodynamic properties are also tabulated in polynomial form [7].

We apply a single-step overall irreversible reaction mechanism in the numerical study:

$$CH_4 \; + \; 2O_2 \; \rightarrow \; 2H_2O \; + \; CO_2, \tag{4}$$

with the reaction rate of methane given by [5]:

$$\dot{\rho}_{CH_4} = -A \rho^{m+n} Y_{CH_4}^{m} Y_{O_2}^{n} \exp(-E_\text{a}/RT). \tag{5}$$

The overall reaction parameters were fit to experiments to predict the correct relation between the burning velocity and flame temperature (for flat adiabatic and burner-stabilized flames) in the range $0.8 \leq \Phi \leq 1.2$ and optimized for $\Phi = 0.8$ [3], leading to $m = 2.8$, $n = 1.2$, $E_\text{a} = 138\text{kJ/mol}$ and $A = 2.87{\times}10^{15}\,\left(\text{kg/m}^3\right)^{1-m-n}\text{s}^{-1}$. The effect of heat losses is incorporated in the fitting procedure to make sure that flame stabilization due to heat transfer to the burner. It was shown in earlier studies [3] that this model accurately describes the global behavior of steady burner-stabilized flames. In [9] it has been shown that this mechanism is also well suited to model the response of one-dimensional lean methane-air flames to low-frequency acoustic distortions. In the current paper we restrict the modeling to premixed methane-air flames with $\Phi = 0.8$.

Only a small part of the repetitive flame structure is computed (a numerical domain with half the pitch width of $(l + d)/2$, using symmetry boundary conditions at

both sides (see Fig.1b)). The inflow part below the burner-plate is also taken into account in the simulations using a flat velocity profile with perturbation, i.e., $u = \bar{u} + u'$ as inflow condition. This procedure accurately models the approaching acoustic wave at the inflow, since acoustic waves have infinite wave length and pressure fluctuations are not needed in the limit of Mach-numbers Ma $\rightarrow 0$ (as used in this model). The outflow is simply modeled using zero derivatives of velocity and other combustion variables, which is also accurate in this case if the outflow boundary is sufficiently far away from the active region.

4 Results

Two types of results are considered in this section. First, the steady flame shape and flame TF is analyzed and compared with numerical results for a flame with $\Phi = 0.8$, $V = 100\,\mathrm{cm/s}$, $d = 2.0\,\mathrm{mm}$ and $l = 3.0\,\mathrm{mm}$ (representative case). A parameter study is subsequently presented for the TF with varying Φ, V, d and l. The typical underlying flame form/size is analyzed and the change in behavior of the flame TF is discussed.

To understand the general structure of the TF of the multi-slit burners presented in this section, it is instructive to consider the flame TF's for a Bunsen-type conical flame and a flat burner-stabilized flame (see Fig.2). As the multi-slit flame contains parts which resemble both these flame patterns, it is expected that the flame TF of multi-slit flames is a weighted sum of the two individual TF's of a Bunsen-type flame cone (flame cone kinematics part) and a flat burner-stabilized flame (flame to burner deck heat-exchange related part). It is well known [2] that the flame TF of a single Bunsen-type flame is characterized by (a) a low-pass filter behavior (amplitude decreasing with frequency, with a cut-off frequency dependent on d), (b) a phase which shows a time delay behavior in the low-frequency range (linearly increasing phase with frequency), which corresponds to a convective wave traveling from the flame foot to the flame tip which takes a time $\tau_0 \propto H/V$ to arrive at the flame front and (c) a slowly varying high-frequency offset behavior (constant gain and phase shift at high frequency). On the other hand, the flame TF of a flat burner-stabilized flame also shows a low-pass filter behavior but shows a limited phase change $\phi(f)$ asymptotically approaching π at high frequencies and displays a large gain $G(f)$ at low frequencies (resonance) [4].

Flame TF for the representative case

Fig.3 compares the steady flame shapes (c) and and TF's (gain G(f) (a) and phase ϕ(f) (b)) for the particular case. The experimental part shows a chemiluminescence photograph while the chemical source term is visualized in the modeling results of Fig.3(c). The correspondence is reasonable despite that different quantities are visualized. The experimental flame has a height of $h = 4.7$mm while the numerically computed flame is slightly smaller with height $h = 4.5$mm. Note also that individual flames stabilize on the slits and do not merge near the foot area in both the experiment and the numerical simulation.

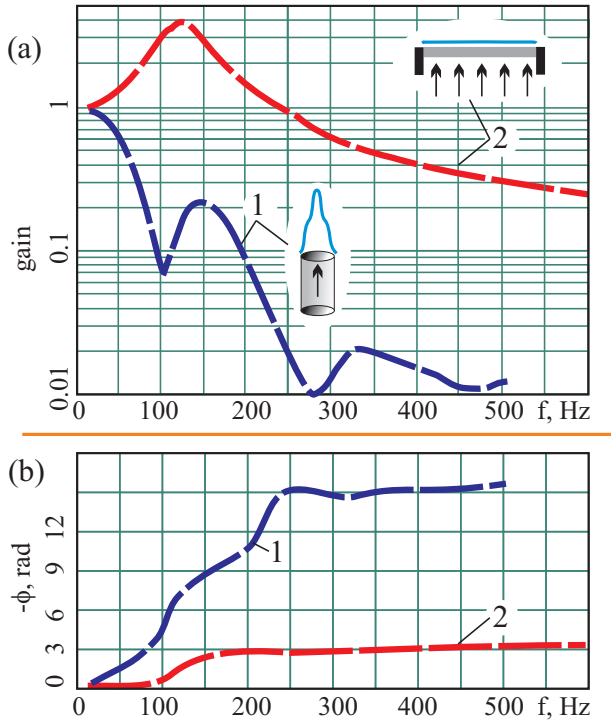

Figure 2: Experimental flame TF gain (a) and phase (b) for a single Bunsen flame on a tube (lines 1 for $\Phi = 0.9$, $V = 150$ cm/s and $d = 1.0$ cm) and a flat flame stabilized on a burner perforated brass deck (lines 2 for $\Phi = 0.9$, V=10 cm/s and T=260C).

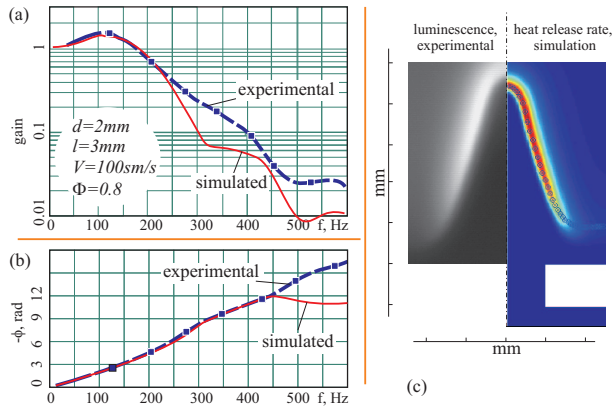

Figure 3: Comparison of experimental and numerical flame TF gain (a) and phase (b) for the representative case including a direct comparison of the steady numerical and experimental flame structure (c). Parameter values are: $V = 100$cm/s, $d = 2.0$mm, $l = 3.0$mm, $\Phi = 0.8$

The experimental and numerical flame TF's are compared in Fig.3(a,b). The correspondence of gain and phase is reasonable. The experimental TF is found by measuring the flame response at a large number of different frequencies, while the numerical result is computed during a single computation, i.e., by modeling the flame response to a small but instantaneous velocity change at the inlet. This perturbation contains the transfer function for all frequencies which can be found by Fourier analysis. It should be noted that the perturbations should be small enough to avoid nonlinear flame

response. This is checked by varying velocity perturbation amplitudes.

A combination of both TF's of a flat flame and a Bunsen-type flame is seen in the case of flames on multi-slit burners (Fig.3). The Bunsen flame (flame cone kinematics) characteristics are very clear, and moreover, we see a larger gain $G(f)$ for low frequencies, corresponding to part of the TF of flat burner-stabilized flames. The effect of the resonant flame foot motion on top of the burner, as found for burner-stabilized flames is visible in terms of a gain $G > 1$ near 100 Hz (see Fig. 3(a)). The fact that the numerical flame TF phase approaches a constant phase of around 4π for $f > 450$ Hz, while the experimental TF phase is still increasing is related to the high sensitivity of the TF phase saturation level to small variations in the flame (mixture) parameters.

Effects of V, Φ, d and l on flame TF

Fig. 4 shows measurements and simulation results of the flame TF for varying V while $\Phi = 0.8$, $d = 2.0$mm and $l = 3.0$mm. The figure indicates that the model is very well capable to predict the behavior of the experimental results for all cases. The TF for the lowest velocities looks very similar to that of the flat burner-stabilized flame (low phase for all frequencies and high gain at small frequencies), since the individual flames are very small and the major part of the combustible mixture is consumed as in a flat surface burner. For higher velocities the flame height increases and much more of the mixture is consumed by the longer Bunsen-type flames, and as a result, the contribution of the Bunsen flame TF to the multi-slit TF increases. Therefore, the phase becomes very similar to the Bunsen-type flame behavior, with constant slope at low frequencies and a saturation at a constant phase at higher frequencies. The slope of the phase (proportional to τ_0) does not change if V is varied, because the flame height H also increases for higher velocities leaving the parameter τ_0 unchanged. The saturation level increases with V like in the case of a single Bunsen flame due to the shift of the cut-off frequency of the low-pass filter to higher frequencies. A similar effect is seen in the gain: at low velocities, $G(f)$ looks like the surface burner gain, while the influence of the Bunsen-type flame gain increases for increasing V. This leads to the observation that the change in gain $G(f)$ is more pronounced than in the case of a single Bunsen flame.

Fig. 5 shows measurement data and numerical results of the flame TF for varying slit width d and distance l with $l/d = 1.5$, while $V = 100$cm/s and $\Phi = 0.8$. Now, the flame height increases (while V remains constant) with increasing d so that the slope of ϕ(f), proportional to $\tau_0 = H/V$ increases. The correspondence between experimental data and numerical results is again excellent.

Fig. 6 shows measurements of the flame TF for varying distance between the slits l while $V = 100$cm/s, $\Phi = 0.8$ and $d = 2.0$mm. Increasing the distance between slits leads to a separation between attachment points of the individual flames, a higher flame foot position and a higher flame height. This, once more explains the increasing slope in the phase plots, while the gain is

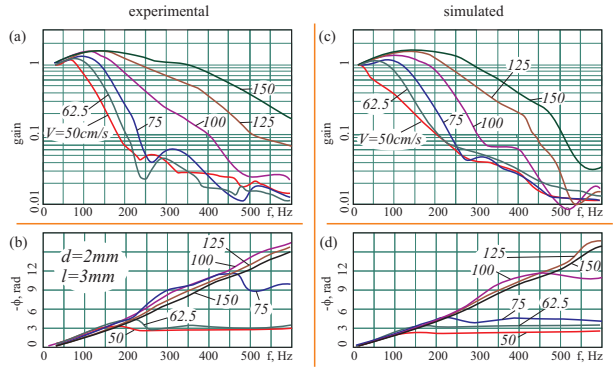

Figure 4: Comparison of experimental flame TF's (a,b) with computed TF (c,d) for varying velocity $V = 50, 62.5, 75, 100, 125, 150$cm/s. Other parameter values are: $d = 2.0$mm, $l = 3.0$mm, $\Phi = 0.8$; TF gain (top, a,c), TF phase (bottom b,d)

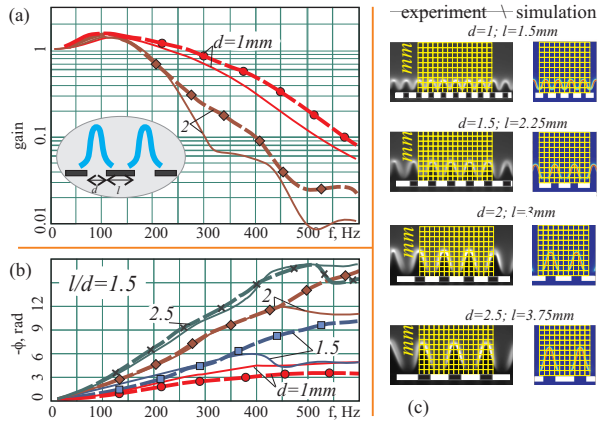

Figure 5: Comparison of measured flame TF (thick lines) with computed TF (thin lines) for varying d and l with $l/d = 1.5$, $V = 100$cm/s, $\Phi = 0.8$; TF gain (top), TF phase (bottom), experimental and numerical steady flame structure (right).

hardly influenced.

Finally, Fig. 7 shows measurements of the flame TF for varying Φ while $V = 100$cm/s, $d = 2.0$mm and $l = 3.0$mm. No comparison with numerical results are given here, since we only did numerical simulations for $\Phi = 0.8$. The slope of the phase $\phi(f)$ is proportional to the convective time $\tau_0 = H/V$ which decreases for increasing Φ simply because the flame length H becomes smaller. A smaller flame is a result of a higher burning velocity associated with a richer mixture. The gain is hardly influenced by changes in Φ as for the case of a single Bunsen flame.

5 Conclusions

Experimental and numerical results of steady flame shape and flame TF are compared for Bunsen-type flames on multi-slit burners. Changes in velocity, slit width and distance between the slits are also considered. The overall agreement indicates that the numerical model, although being simple in terms of chemical kinetics, is able to describe the full dynamics of the system. The comparison also gives additional confidence in the meth-

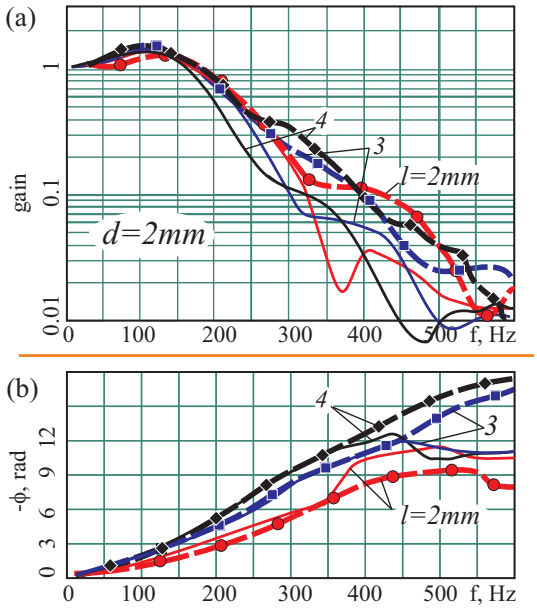

Figure 6: Comparison of measured flame TF (thick lines) with computed TF (thin lines) for varying l and constant $d = 2.0$mm with $V = 100$cm/s, $\Phi = 0.8$; TF gain (top), TF phase (bottom))

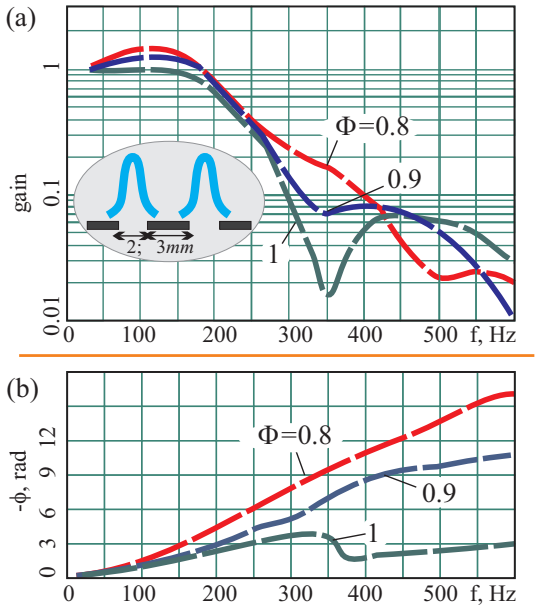

Figure 7: Measured flame TF for varying equivalence ratio Φ with $V = 100$cm/s, $d = 2.0$mm, $l = 3.0$mm TF gain (top), TF phase (bottom)

ods (i.e. chemiluminescence and heated wire techniques) used during the experimental research.

The results indicate that the TF of multi-slit flames is a weighted sum of the well-known TF's of a Bunsen-type conical flame and that of a flat flame stabilized on a flat burner. If the flames are short, the full multi-slit TF is similar to the TF of burner-stabilized flames because only a small part of the mixture is consumed by the small Bunsen flames. The opposite is true in the case of long Bunsen-type flames: the major part of the mixture then is consumed by longer flames, leading to a TF very similar to that of the corresponding Bunsen-type flame.

References

[1] M. Fleifil, A.M. Annaswamy, Z.A. Ghoneim and A.F. Ghoniem, Response of a laminar premixed flame to flow oscillations, *Combust. Flame* 106, 487-510 (1996).

[2] V.N. Kornilov, K.R.A.M. Schreel and L.P.H. de Goey, Experimental assessment of the acoustic response of laminar premixed Bunsen flames, *Proc. Combust. Inst.* 31, 1239-1246 (2007).

[3] H.C. de Lange and L.P.H. de Goey, Two-dimensional methane/air flames, *Combust. Sci. Tech.* 92, 423–427 (1993).

[4] R. Rook, *Acoustics in Burner-Stabilised Flames*, PhD Thesis, Eindhoven University of Technology (2001).

[5] W.E. Kaskan, The dependence of flame temperature on mass burning velocity, *Sixth Symp. (Int.) on Combustion*, The Combustion Institute, New Haven, pp. 134–143 (1956).

[6] R.J. Kee, G. Dixon-Lewis, J. Warnatz, M.E. Coltrin, and J.A. Miller, *A Fortran computer code package for the evaluation of gas-phase multicomponent transport properties*, Sandia National Laboratories, SAND86-8246 (1986).

[7] R.J. Kee, F.M. Rupley, and J.A. Miller, *The chemkin thermodynamic database*, Sandia National Laboratories, SAND87-8215 (1991).

[8] A.A. Putnam, *Combustion Driven Oscillations in Industry*, Elsevier, New York (1971).

[9] R. Rook, L.P.H. de Goey, K.R.A.M. Schreel, and R. Parchen, Response of burner-stabilized flat flames to acoustic perturbations, *Combust. Theory Modelling* 6 (2), 223-242 (2002).

[10] T. Schuller, S. Ducruix. D. Durox and S. Candel, Modeling tools for the prediction of premixed flame transfer functions, *Proc. Combust. Inst.* 29 , 107-114 (2002)

[11] M.D. Smooke and V. Giovangigli, Formulation of the premixed and nonpremixed test problems, in: *Reduced kinetic mechanisms and asymptotic approximations for methane-air flames*, ed. M.D. Smooke, pp. 1-28, Springer, Berlin (1991).

[12] B. van 't Hof, *Numerical Aspects of Laminar Flame Simulation*, PhD Thesis, Eindhoven University of Technology (1998).

[13] B. van 't Hof, J.H.M. ten Thije Boonkkamp and R.M.M. Mattheij, Pressure Correction for Laminar combustion Simulation, *Combust. Sci. Tech.* 149, 201–223 (1999).